Soft Matter

PAPER

View Article Online
View Journal | View Issue

Cite this: *Soft Matter*, 2026, **22**, 1376

Effect of polymer binder on dispersion stability of dense non-colloidal pastes

Alexandra A. Dobbs,[a] Nora O'Kelly,[b] Laurel A. Hilger,[b] Victor Breedveld[a] and Blair K. Brettmann*[ab]

Improving the processing of dense paste composites is pivotal for production of material formulations that consistently meet performance criteria, integrate with new technologies, and are environmentally conscious. There is a need in the field to define formulation–processing relationships that can be leveraged to support the formulation development and processing of dense pastes. The key challenge of interest to this work is the formation of heterogeneities in the particle spatial distribution during processing. Dense pastes undergo particle network deformation under the complex shear and pressure forces experienced during processing. Gravitational forces and applied stresses that exceed the viscoelastic yield stress can cause irreversible particle migration and the formation of heterogeneous particle microstructures. Such heterogeneities, if persistent after solidification into the final composite, may affect mechanical properties and performance. Herein, the influence of polymer molar mass on heterogeneity formation during paste processing is evaluated *via* settling experiments and rheological testing. The effects of polymer molar mass are deconvoluted from the effects of viscosity using viscosity-matched binder solutions of aqueous polyvinylpyrrolidone or polyethylene oxide and bimodal suspensions of non-colloidal glass particles with a total solids content of 61.4 vol%. We show that low molar mass binders at high concentrations provide improved stability against settling and shear induced migration, which is attributed to balanced viscous dissipation and elasticity. Elucidating the formulation-processing relationships between polymer formulation parameters and paste stability during processing provides insight into the complex rheology of dense pastes, and enables informed polymer selection during formulation development.

Received 20th October 2025,
Accepted 19th January 2026

DOI: 10.1039/d5sm01059d

rsc.li/soft-matter-journal

Introduction

Dense pastes are multicomponent materials that are vital to an array of applications including solid-state electronics,[1] pharmaceuticals,[2] energetic materials,[3] and construction.[4] They are soft materials that contain >50 vol% solid particles suspended in a fluid containing polymers, pre-polymers, solvents, and/or additives, and are often solidified downstream in processing to create functional composite materials. The continuous phase of both the soft paste and the hardened composite is generally referred to as the binder, as its purpose is to bind particles together. Dense pastes are notoriously difficult to process due to their high particle contents and multiphase interactions that result in highly viscous materials with non-Newtonian, pseudoplastic flow behavior.[5–10] Processing challenges both slow down production rates and compromise the properties of the final product.

The viscosity and flow behavior of the paste is dictated by formulation factors, such as solids content,[10–12] particle size distribution,[10,13,14] and polymer selection.[10,15] Formulation-processing relationships are critical for the design of highly loaded particle composites as such knowledge can be leveraged to guide formulation development and overcome processing challenges. Processability can be defined by paste flowability,[9,16,17] shape retention,[6] and stability. Flowability is the ability of the paste to deform (yield) and shear thin under applied forces and dictates ease of extrusion[18,19] and mixing.[15,20] Shape retention refers to the ability of the paste to maintain a desired shape after extrusion and is dependent upon the structural strength of the paste.[4] Weak pastes will yield/slump after extrusion under gravitational forces[14] or under the weight of additional layers of material.[4] Stability is a term used to describe a suspension's ability to maintain, or re-attain homogeneity after a disturbance. In some cases, homogeneous pastes can be achieved after mixing, but heterogeneities may begin forming immediately afterwards.[5] Heterogeneities include any non-uniformities in

[a] *School of Chemical and Biomolecular Engineering, Georgia Institute of Technology, Atlanta, GA, USA. E-mail: blair.brettmann@chbe.gatech.edu*
[b] *School of Materials Science and Engineering, Georgia Institute of Technology, Atlanta, GA, USA*

the spatial distribution of the dispersed particles throughout the bulk of the material. Mechanical and chemical properties of the final product are highly dependent upon inter-particle proximity, and microstructural control is thus imperative for achieving and reproducing the desired product performance.[10,21] Formulating processable dense pastes is challenging as efforts towards improving stability and shape retention, such as increasing viscosity and yield strength, can negatively impact flowability. Dense paste stability against heterogeneity formation has not been studied in the context of processing as thoroughly as flowability and shape retention. This is because it does not necessarily inhibit processing,[22] but rather creates processing challenges such as nozzle clogging,[23] inconsistent extrusion,[14] and the need for multiple mixing cycles.[3]

Mixtures containing non-colloidal particles at high particle loadings have a strong tendency to form heterogeneities during flow or under other forces. The root cause of heterogeneity formation during processing is irreversible particle rearrangement. The most common mechanisms of heterogeneity formation are settling under gravity and particle migration under shear forces.[24–28] Non-colloidal dispersions cannot be stabilized *via* electrostatic or thermal forces and will begin to settle immediately after mixing. Size segregation also occurs during settling as coarse particles settle faster than fine ones. Settling rates are determined experimentally by imaging the segregation of formulation phases over time, and can be estimated using mathematical models for hindered settling.[29–34] Rheological tests measuring storage and loss modulus as a function of oscillation frequency amplitude are also used as an indirect, but fast way to elucidate settling stability.[35]

Shear-induced migration occurs when particles non-uniformly rearrange under complex shear and pressure forces, then become locked in segregated, agglomerated, or jammed 3-dimensional particle networks. Heterogeneities that form due to shear induced migration include binder filtration,[36] size segregation,[37] slip layer formation,[38,39] and agglomeration.[40,41] Direct observations of shear-induced migration can be accomplished using advanced imaging techniques, but can suffer in accuracy at high particle concentrations where tracer particle tracking and complex velocity fields require special attention.[42,43] Conversely, the effects of shear induced migration can be observed in the final product after the binder is solidified using solid-state imaging techniques, such as micro-CT or SEM. It is important to note that for these and other characterization methods, it is not merely the shear-induced migration being captured, but also effects from settling, loading history, *etc.*, which are difficult to deconvolute in dense pastes. Rheological techniques do not provide direct measurements of particle spatial distribution, but instead measure how changes in the particle microstructure impact bulk properties. It is generally understood that bulk rheological properties are directly dependent on the particle microstructure and can be related to particle spatial rearrangements under shearing forces. For example, in some cases vorticity-oriented particle agglomeration can be measured as pressure forces exerted on surfaces normal to the direction of flow.[41] While the chaotic flow of particle segregation is scientifically interesting, it is generally undesirable in dense paste processes.

One difficulty in working with dense pastes lies in the range of heterogeneity formation mechanisms that may need different stabilization approaches. Efforts to stabilize non-colloidal particle pastes against heterogeneity formation must minimize the degree of particle settling and shear-induced migration during processing as particle rearrangements are driven by inertial forces.[44] The majority of studies on heterogeneity formation and stability of dense pastes focus on the effects of particle properties, and less attention has been given to the properties of the binder. However, significant prior work has addressed the effect of polymer molar mass and concentration in the continuous phase on shear-induced migration and settling of dilute suspensions and lower solids content slurries of non-colloidal particles.[45–49] These have shown that higher polymer concentrations and/or molar masses led to a greater degree of particle interactions (tendency to collide) during settling[45,46] and shear induced migration of particles to the centerline or wall during shear flow.[49] Overall, studies investigating the effects of molar mass and concentration on settling and shear induced migration in lower solids content suspensions attribute heterogeneity formation to either viscous shear thinning and/or elasticity of the fluid continuous phase.

The impacts of the interstitial fluid in dense pastes of non-colloidal particles are thought to diminish when particle loading approaches the maximum packing fraction and particle dynamics are largely controlled by geometrical constraints.[50,51] Interestingly, the polymer molar mass/concentration of the continuous phase can still influence stability in high particle loading suspensions, and these relationships are typically investigated *via* rheological techniques. The effect of the molar mass of polyvinyl pyrrolidone (PVP) on processability of dense pastes has been characterized by the critical onset shear thickening stress[52] and paste viscosity,[11] with rheological tests being used to gain some insight into the role of the polymer and its ties to extrudability. Similarly, others have looked at polymer molar mass for polymers such as polyethylene oxide (PEO),[53] xanthan gum,[35] carboxymethyl cellulose (CMC),[35] polynaphthalene sulphonate (PNS),[54] and polycarboxylate ether (PCE)[54] with rheological tests and processing parameters, but none have separated the effect of molar mass or concentration from binder viscosity; thus, the observed effects may primarily stem from differences in viscosity, as both concentration and molar mass impact the viscosity of the polymer solution.

The molecular characteristics of the continuous phase have critical implications on the stability and processability of dense pastes; however, this is often overlooked during formulation. Properties such as molar mass and concentration are typically selected for their impacts on mechanical properties and paste viscosity, and less attention is given to stability against heterogeneity formation. To the best of the authors' knowledge, there are no studies that distinguish between the effects of molar mass and concentration on stability, deconvoluted from the effects of viscosity. The present study aims to address this knowledge gap by characterizing the settling and shearing

stabilities of dense pastes formulated with high and low molar mass PVP and PEO solution-based binders. Polymer concentration is tuned to create viscosity-matched solutions as the dispersing phase for the particles, thus deconvoluting the effects of binder viscosity from polymer molar mass. This work demonstrates how polymer molar mass and concentration can be modified to improve stability independent of solution viscosity, thus providing formulation processing relationships relevant to the production of high-quality pastes and composite materials.

Experimental methods

Materials

Solid Spheriglass® (soda lime) glass spheres with diameters of 117–216 μm (A-Glass 2024) and 4.3–17 μm (A-Glass 5000) were purchased from Potters Industries. Particle sizes were measured using a Malvern Instruments Mastersizer 2000SM Particle Size Analyzer with a Hydro 2000SM (AWM2002) Dispersion Unit, and are reported in SI, Fig. S1. PVP with weight average molar mass of 55 kg mol^{-1} and 1300 kg mol^{-1} and PEO with number average molar mass 20 kg mol^{-1} and 2000 kg mol^{-1} were purchased from Millipore Sigma.

Sample preparation

Aqueous polymer binder solutions were prepared in large batches by combining the appropriate ratio of polymer to DI water, then mixing on a shaker table until the polymers were fully dissolved. All vessels were sealed with two layers of parafilm to prevent solvent evaporation. All pastes were prepared by combining a total volume fraction of ϕ = 61.4 vol% glass beads with the polymer binder in 20 mL glass vials, then mixing in a Flacktek SpeedMixer for 30 seconds at 1000 rpm followed by 150 seconds at 1500 rpm. The particle phase consisted of two particle sizes that were manually mixed together at a coarse to fine volume ratio of 71 : 29 or 65 : 35, as determined by assuming a nominal density of 2.5 g mL^{-1} for both particles. A particle volume fraction of ϕ = 61.4 vol% glass beads was selected based on prior work that identified it as a flowable fraction for 3D printing.[11,14] The mixing process with the SpeedMixer was selected based on prior work that determined adequate times and speeds for distributive mixing (wetting), followed by dispersive mixing that ensured homogeneity (analyzed as viscosity change) and minimized temperature rise.[11]

Settling tests

Pastes were prepared with a small amount of dye (<0.15 vol%, Procion®) in the continuous phase to increase the visibility of segregation. Immediately after mixing, a mark was made on each vial to visually distinguish the fill level from residue that was smeared on the vial walls due to high shear mixing. The vials were then transferred to a light box, and images were taken periodically over a 74-hour settling period. As particles settled, the separation of particle-rich and binder-rich phases became apparent as the binder, dyed blue, contrasted with the opaque particles. Scale bars were affixed to the vials before mixing and the length of the segregated layers was measured using ImageJ. A wooden block stage and a camera stand were used to ensure consistent placement and camera angles across replicate measurements. A photo of the experimental setup is included in SI, Fig. S2.

Rheological characterization

Rheological experiments were conducted on a TA Instruments Discovery Hybrid Rheometer-3. All experiments were temperature controlled at 25 °C, and solvent traps were used to mitigate solvent evaporation. A double wall concentric cylinder with a solvent trap was used for measurements of the fluid binders without particles. For rheological testing of pastes, 200-grit sandpaper was secured to 20 mm Peltier plates as this was found to be an effective means of mitigating slip (SI, Fig. S3). The solvent well was filled with water and a solvent trap was used to create a solvent-saturated environment and suppress solvent evaporation.[55] The operating gap was set to 1 mm.

The viscosity of the polymer binder solutions was measured as a function of shear rate from 0.1 s^{-1} to 50 s^{-1}. Zero-shear viscosity (η_0) values were calculated by fitting the viscosity data to the Carreau–Yasuda model (SI, eqn (S1)). All binder solutions were formulated at concentrations above the critical entanglement concentration, c_e, which was determined from measurements of zero-shear viscosity at various polymer concentrations, as shown in Fig. S4. Small amplitude oscillatory strain sweeps were performed to identify viscoelastic yielding transitions such as the linear viscoelastic region (LVR), as illustrated in Fig. 1a. All oscillatory measurements were conducted at a frequency of 10 rad s^{-1}, a common frequency for such testing.[56] The material property of interest measured during these tests is the storage modulus as it is primarily influenced by elastic particle–particle interactions.

Three-interval thixotropy (3IT) testing was used to assess the transient particle structure evolution and quantify suspension stability.[55,57–62] This technique exposes the specimen to three intervals of shearing forces in order to measure the recovery of its viscoelastic properties after being deformed beyond the yield point (beyond the LVR), typically under case-dependent processing conditions (Fig. 1b). The first and third intervals (rest and recovery) of three-interval thixotropy tests were conducted in oscillatory mode at 0.01% and 10 rad s^{-1} frequency, which is within the LVR for all samples, and will not give rise to shear induced migration effects.[63] The second interval (breakdown) was conducted in rotational mode at 40 s^{-1} as this is analogous to shear rates experienced during shaping processes such as extrusion. Resting and breakdown interval conditions were held for 120 and 100 s, respectively, and recovery was measured over 2 hours.

The three intervals are (1) rest, (2) breakdown, and (3) recovery. In interval one (rest), small deformations (low strains) within the LVR are applied to establish starting properties. In interval two (breakdown) the sample is exposed to high shears beyond the LVR that significantly disrupt the established structure. In interval

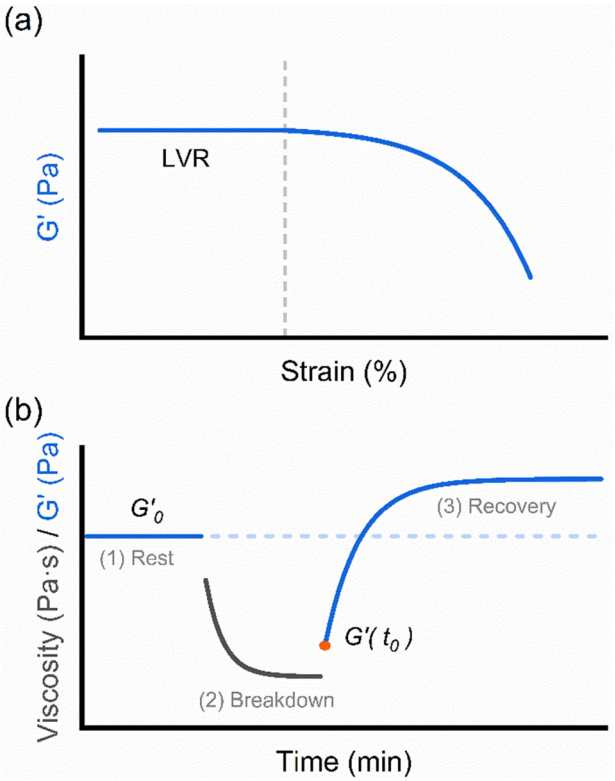

Fig. 1 Illustration of oscillatory strain sweep (a) and three-interval thixotropy (3IT), (b) data. Oscillatory strain sweeps show storage modulus, G', as a function of strain deformation. G' is not dependent upon strain within the linear viscoelastic region, and the vertical line represents the yielding transition. 3IT tests track G'/viscosity as a function of time, t, under alternating shearing conditions. The three lines represent the three shearing intervals, (1) rest at 0.01% oscillation strain (measure G'), (2) breakdown at 40 s^{-1} (measure viscosity), and (3) recovery, again, at 0.01% oscillation strain (measure G').

three (recovery) low strains are re-applied and the evolution of rheological properties over time are measured over a period of structural recovery. An ideally thixotropic material will eventually reach a steady state at 100% recovery, meaning the steady state properties at the end of recovery match those of the initially homogeneous suspension.

The storage modulus was evaluated over time during the 3IT tests because it is a measure of paste elasticity, and particle interactions in the matrix are expected to significantly impact paste elasticity. During recovery (third interval), the storage modulus continuously increases over time as particle–particle contacts re-form after being disrupted in the second interval, and the paste ages.[64] Differences between initial (dashed line in Fig. 1b) and recovered storage modulus are expected to correlate to heterogeneity formation. Thus, we calculate the recovery of the storage modulus in interval three (% Recovery) over time through eqn (1).

$$\%\ \text{Recovery} = 100 \times \frac{\log(G'(t)) - \log(G'(t_0))}{\log(G'_0) - \log(G'(t_0))} \qquad (1)$$

% Recovery represents the ratio of initial and recovered storage modulus. Storage modulus evolution over time during structural recovery, $G'(t)$, is normalized by the storage modulus of the initially homogeneous paste from interval one, G'_0. $G'(t)$ is shifted by the storage modulus directly after breakdown occurs, $G'|_{t\to 0} = G'(t_0)$, such that % Recovery is zero at t = 0; and G'_0 is shifted accordingly to maintain the scaling relationship.[58] Calculated values of % Recovery can exceed 100% if the sample reaches greater elastic modulus after shear compared to its original state, such as illustrated in Fig. 1b.

Pre-shearing is typically conducted at high shear rates and is intended to erase the shear history from sample loading. In our work, pastes were pre-sheared under small amplitude oscillations approximately 10% outside of the linear viscoelastic region for 100 s followed by a 300 s conditioning interval as this was found to be an effective method for pre-shearing and avoided high shear rates which can impact particle dispersion (SI, Fig. S5). Given the small amplitudes and low shear used for the pre-shear procedure, we do not expect that the initial paste microstructure for the sedimentation tests, which were performed in the same vials used for mixing, will be significantly different from the structure of the pastes tested for rheological properties.

Results

To study the influence of polymer molar mass on heterogeneity formation independent of viscosity, we first need to develop appropriate model formulations. Ideal model pastes are formulated with materials that have highly controlled properties, are free of convoluting effects, have high particle loadings, and cover an appropriate range of parameters. With this in mind, a series of dense paste formulations with bimodal particle distributions and viscosity-matched polymer binders were investigated; compositions of the formulations are displayed in Table 1.

In this study, the term 'binder' refers to the dispersing phase, the polymer solution comprised of both polymer chains and solvent molecules. It should be noted that in other studies binder may refer to the solidified polymer. To test the effects of polymer molar mass (independent of solution viscosity), PVP and PEO polymers with molar masses of $\sim 10^4$ and 10^6 g mol^{-1} (10 and 10^3 kg mol^{-1}) were compared. A two-order-of-magnitude

Table 1 Formulations of dense pastes with viscosity matched polymer binders

Polymer[a]	Binder composition[b]	Coarse : fine ratio[cd]
PVP	16 wt% 1300 kg mol^{-1}	71 : 29
		65 : 35
	44 wt% 55 kg mol^{-1}	71 : 29
		65 : 35
PEO	1.7 wt% 2000 kg mol^{-1}	71 : 29
		65 : 35
	39 wt% 20 kg mol^{-1}	71 : 29
		65 : 35

[a] Polymers dissolved in DI water. [b] Concentration was tuned to attain a solution viscosity of 0.65 Pa s. [c] Coarse particles are 159 μm, fine particles are 8.7 μm (d_{50}). [d] Total solids loading is ϕ = 61.4 vol%.

difference between the high and low polymer molar masses was chosen to better isolate the effects of molar mass, as commercial polymers are known to have significant chain length dispersities,[65] which can bias rheological behavior. Water was selected as the solvent to mitigate solvent evaporation, which can alter time-dependent experiments. Examples of the transient effects of solvent evaporation are provided in SI, Fig. S6.

The concentrations of high and low molar mass polymers for both PVP and PEO dissolved in water were adjusted to achieve viscosity-matched solutions with a target zero-shear viscosity for all solutions of approximately 0.65 Pa s, similar to binder viscosities reported in previous studies.[11,14] Binder compositions are presented in Table 1, and shear viscosity profiles may be found in SI, Fig. S7. Viscosity profiles demonstrate close agreement (within < 0.1 Pa s) between each solution.

Spherical glass beads were used to mitigate behavior that may arise due to particle aspect ratio, surface roughness, and size dispersity; formulation factors with significant effects on paste properties.[5] The aspect ratio and surface roughness of the glass beads were qualitatively assessed from SEM imaging (Fig. S8), and size distribution data can be found in Fig. S1. Fine particles that are at least seven times smaller than coarse particles act as lubricants and can improve particle packing efficiency, thus allowing for higher particle loadings. The total particle loading was kept constant at 61.4 vol%, as this is well below the jamming transition of 67 vol% found in a previous study.[11] Bimodal particle distributions of 65 vol% coarse (159 μm) with 35 vol% fine (8.7 μm) particles, and 71 vol% coarse with 29 vol% fine particles (henceforth denoted as 65 : 35 and 71 : 29) were chosen to investigate the effects of the coarse to fine volume ratio at the same total solids content.

The first stability phenomenon we investigated with these model suspensions is particle settling as settling can occur immediately after mixing and can impact paste properties during storage and processing. For many suspensions with low particle loadings, Stoke's law—which is based on a particle of a given size and mass settling due to gravity in a Newtonian fluid—is used to predict the settling rate. However, in dense pastes, the other particles in suspension slow settling and necessitate the use of a hindered settling model.[5] Although improved with respect to consideration of particle interactions, the majority of available hindered settling models use the zero-shear viscosity of the binder, which is an oversimplification for non-Newtonian continuous phases like most binders.[34] Here we examine the settling of model formulations that have the same binder viscosity but different molar mass polymers, specifically measuring how the thickness of the binder-rich top layer increases with time. A binder rich layer forms at the top of the suspension as particles settle to the bottom of the container; this layer can be clearly seen through changes in paste color and opacity. Analysis of the growth of this segregated layer as a function of time allows us to assess the influence of polymer molar mass and concentration in the continuous phase on the severity of the heterogeneity formation in the paste.[66]

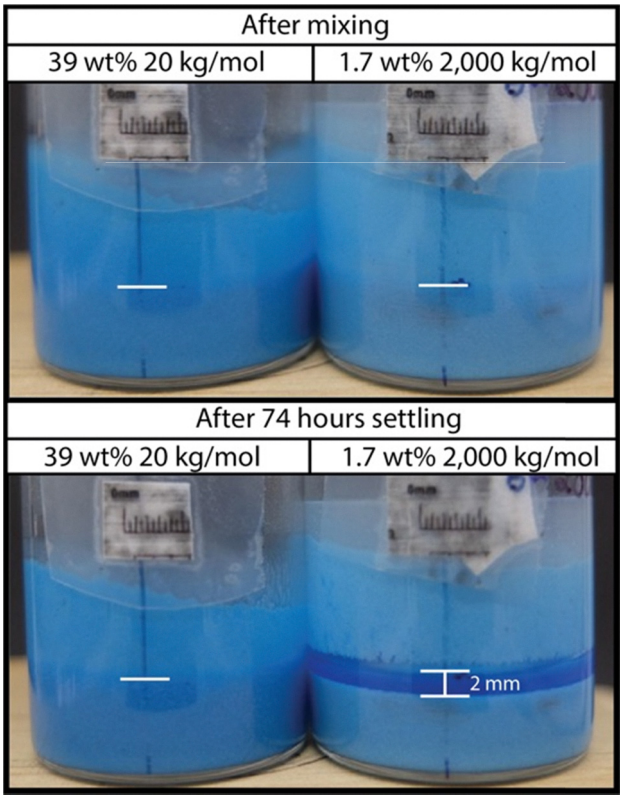

Fig. 2 Images of vials taken directly after mixing (top) and after settling for 74 hours (bottom). The left-hand vial contains the 39 wt% 20 kg mol^{-1} PEO binder and the right-hand vial contains the 1.7 wt% 2000 kg mol^{-1} PEO binder, both formulated with the 71 : 29 volume ratio of coarse to fine particles. Scale bars were secured to the front of the vials. The top white line on the vial marks the original fill level, and the bottom line in the 1.7 wt% 2000 kg mol^{-1} vial (bottom right) is the top of particle rich phase after 74 hours.

Fig. 2 shows representative images of vials immediately after mixing and after 74 hours sitting undisturbed in a light box for pastes formulated with the 39 wt% 20 kg mol^{-1} PEO binder (left) and the 1.7 wt% 2000 kg mol^{-1} PEO binder (right) at a 71 : 29 volume ratio of coarse to fine particles. Horizontal lines were added to the vials to mark the fill level of the paste, which is obscured by residual smearing along the vial wall after high shear mixing. The images taken directly after mixing show that the two pastes appear visually homogeneous. After 74 hours the high molar mass formulation (right) forms a 2.0 mm tall binder-rich layer, while the low molar mass formulation (left) remains unchanged. This indicates that the severity of particle settling in dense pastes can vary independent of binder viscosity. The images in Fig. 2 are representative images for PEO based formulations at two time points and provide visualization of the severity of segregation for this specific formulation. We used these and additional images to measure the thickness of the binder rich layer over time for all model formulations to study in more detail how the polymer molar mass impacts stability against settling in dense pastes.

Fig. 3 shows the thickness of the binder rich phase that forms on top of the paste over time for all model formulations

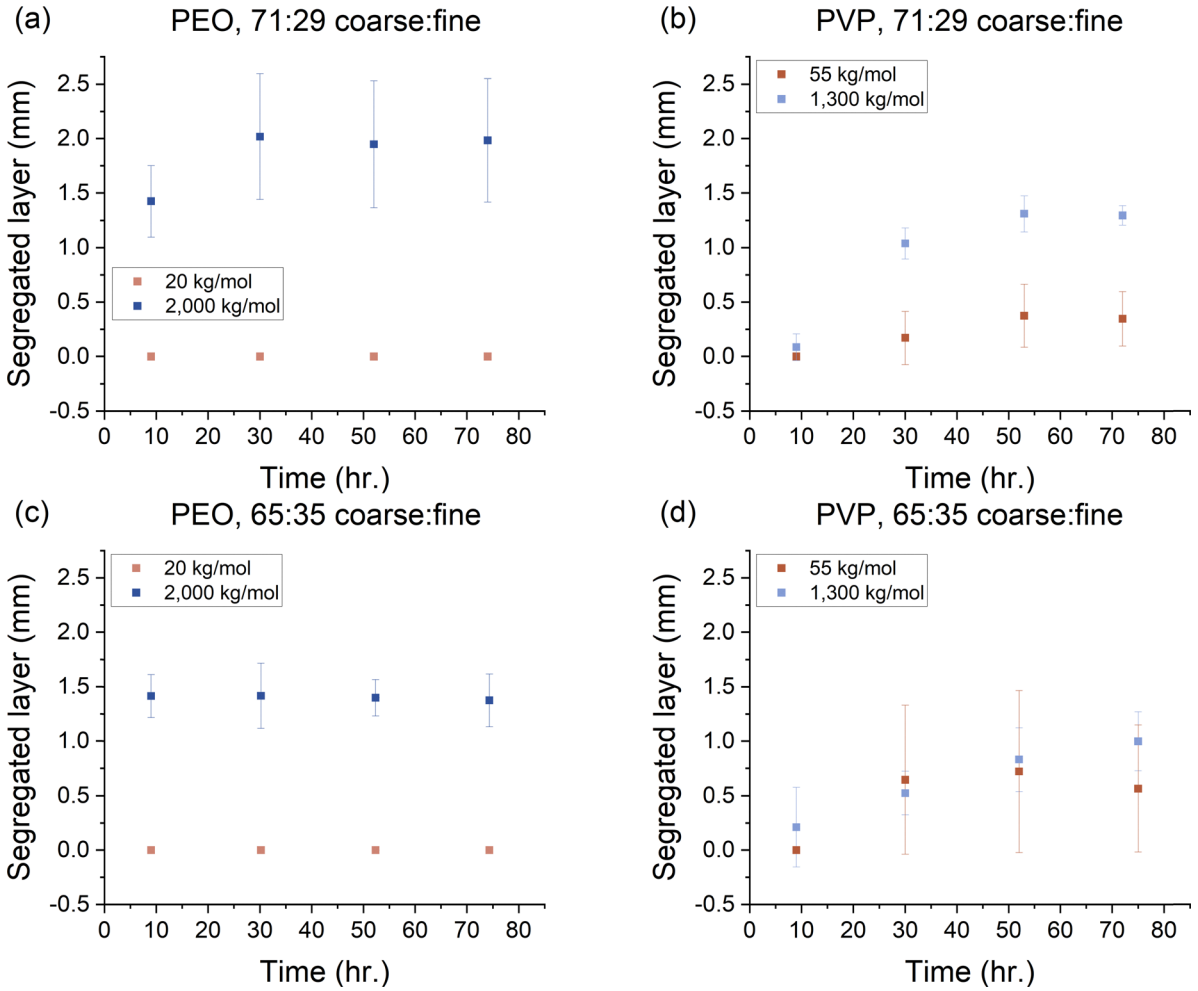

Fig. 3 Segregation of the binder rich phase from the bulk due to settling over time for viscosity matched PEO (a) and (c) and PVP (b) and (d) binders with a coarse to fine particle volume ratio of 71 : 29 (a) and (b) and 65 : 35 (c) and (d). Error bars represent one standard deviation of four replicates for the 55 kg mol^{-1} PVP and 65 : 35 coarse to fine particle ratio formulation and three replicates for all other systems.

listed in Table 1. The severity of particle settling can be assessed by analyzing the thickness of the binder rich layer after 74 hours. Interestingly, for the pastes containing the 71 : 29 volume ratio of coarse to fine particles (Fig. 3a and b), both PVP and PEO high molar mass formulations show thicker binder-rich layers compared to their low molar mass counter parts. The high molar mass PVP system develops a 1.3 mm layer while the low molar mass formulation generates a 0.3 mm layer. Similarly, the high molar mass PEO system results in a segregated layer of approximately 2.0 mm thick, while the low molar mass PEO system results in no segregation. These results indicate that short chain polymers at high concentrations may provide a stabilizing effect against settling, which is in contrast to the findings of Adjou *et al.*[54] However, in their work the polymer solutions did not have the same viscosity, so the improvement of stability with increasing polymer molar mass is likely due to the increase in binder solution viscosity.[54] Here we see that, for a given viscosity, the molar mass and/or concentration of the polymer impacts the pastes stability against settling. Interestingly, the polymer solutions are all nominally Newtonian up from 0.1 to 5 s^{-1} shear rates (and in some cases across the entire range tested, SI, Fig. S7a), indicating that it is the viscoelasticity of the dense paste more than the polymer solution leading to this different behavior with molar mass. This is an important observation, as amongst the many models used for hindered settling in highly concentrated dense pastes, the only formulation factors are solution viscosity, particle size distribution/ratio, and total particle loading, all of which are kept constant in these experiments.[34] Instead, it points to an important role of interactions in this complex mixture that are enhanced by having a higher molar mass polymer.

The results presented in Fig. 3a and b were for a particle mixture that has a lower fine particle content and a higher coarse particle content. Fine particles that fit within interstitial voids between coarse ones have been shown to impact both settling and shearing stability in dense pastes.[14,50,66] In order to investigate the effects of increasing fine particle content without changing total particle loading, we compared the settling rates of pastes formulated with a coarse to fine volume ratio of 71 : 29 to formulations with a ratio of 65 : 35.

Fig. 3c and d show the thickness of the segregated binder-rich layer as a function of time for the same polymer binders but with the 65 : 35 volume ratio of coarse to fine particles. We can see that the stabilizing effect observed for low molar mass polymers is not observed for the 65 : 35 PVP systems (Fig. 3d), as the settling rate and total amount of binder segregation is the same between the high and low molar mass formulations. However, the PEO systems, Fig. 3c, show that the segregated layer formation behavior is very similar to that of the 71 : 29 (Fig. 3a) particle mixture. The high molar mass PEO sample with the decreased fine particle content appears to have a slower settling rate and also compacts/settles more under gravity, leaving a thicker fluid layer, compared to the formulation with more fine particles. While the results for the PVP solutions are consistent with the hypothesis that the polymer molar mass and/or concentration matter more for low fine particle contents, the PEO systems still see differences in the stabilizing effect at both compositions, indicating a more complex relationship. These results suggest the influence of molar mass on segregation behavior is, to some extent, particle content dependent, but that its impact depends on the specific polymer.

In addition to binder separation from settling, particles in dense pastes can also undergo shear-induced migration leading to heterogeneity formation, and we expect that the binder will also play an important role in stabilizing against this phenomenon. Here we use 3IT tests to disrupt the paste's particle microstructure using shear forces, then observe the recovery of particle contacts over time, using a sufficiently long recovery time interval to capture the immediate effects from shear-induced migration and longer effects from that and other paste aging phenomena. We again use the viscosity matched binder formulations to determine whether the greater stability provided by the low molar mass polymer that was observed during settling would translate to stability against shear induced migration and aging. Fig. 4 shows the relative change in storage modulus (% Recovery) over a 2-hour recovery period after shearing the pastes at 40 s^{-1} for 100 s. Each curve

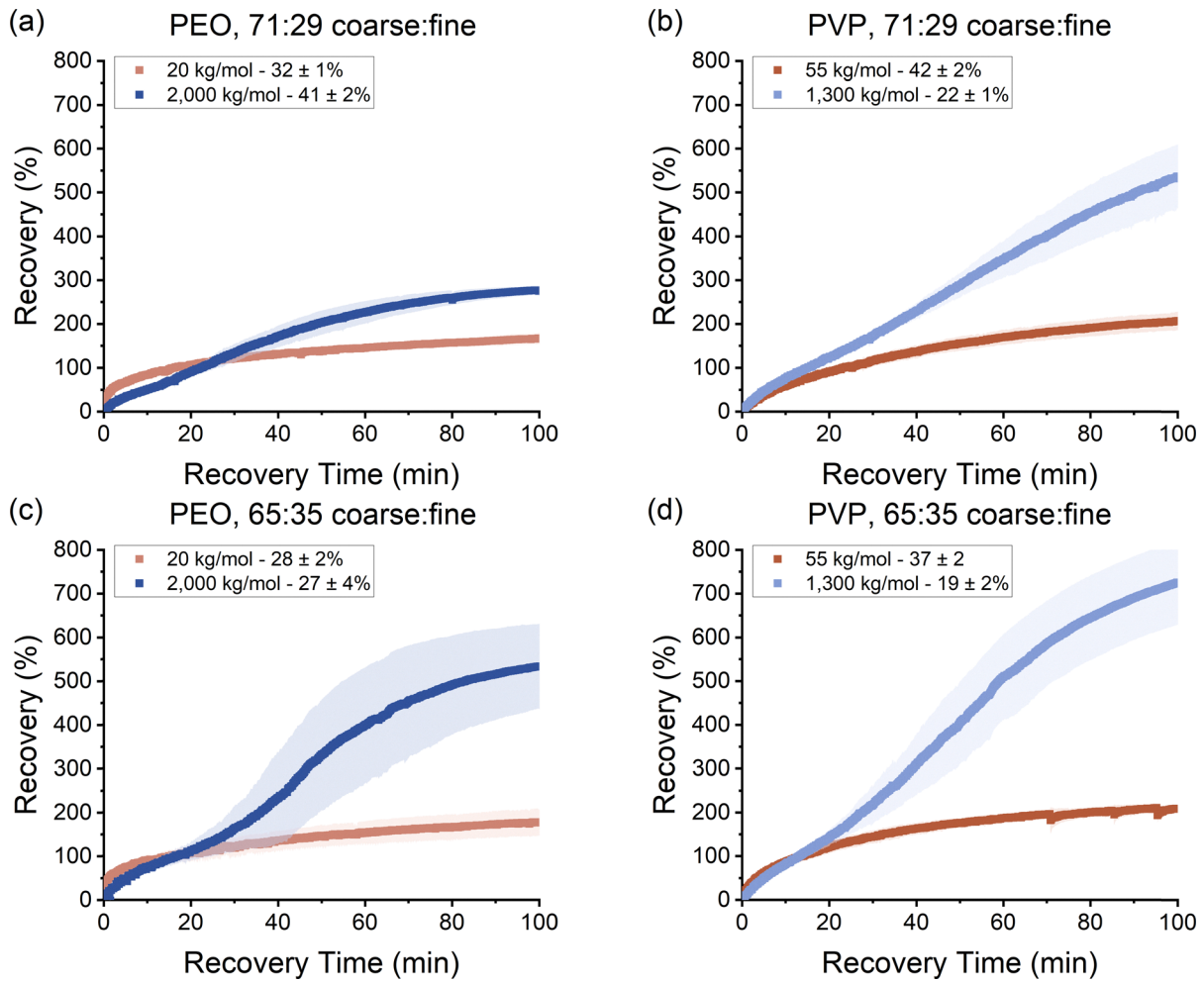

Fig. 4 Effects of polymer binder molar mass on structural recovery of dense pastes over time. Volume ratios of coarse to fine particles are 71 : 29 (a) and (b) and 65 : 35 (c) and (d). Binders tested are PEO at 20 and 2000 kg mol^{-1} (a) and (c) and PVP at 55 and 1300 kg mol^{-1} (b) and (d). The initial difference between the pre- and post-shear values of G' (in %) are listed in the legends, and the shaded regions indicate uncertainty to one standard deviation of three replicate measurements.

is shifted by the initial difference between the pre- and post-shear modulus (*i.e.* all curves start at 0% recovery); for reference, the initial drops in storage modulus due to shear are reported in the figure legends for all samples.

The deviation from 100% recovery is the relative difference between pre- and post-shear properties and indicates the severity of heterogeneity formation. Transient recovery profiles for the 71 : 29 volume ratio of coarse to fine particle formulations are shown in Fig. 4a and b. For the PEO formulations, the final recovery is 280 ± 20% for the high molar mass paste and 170 ± 10% for the low molar mass paste (Fig. 4a). The final recovery values are 560 ± 70% and 210 ± 20% for the high and low molar mass PVP formulations, respectively (Fig. 4b). For mixtures with a 65 : 35 volume ratio of coarse to fine particles and the PEO binders, the final recovery was 180 ± 30% for the low molar mass paste and 540 ± 90% for the high molar mass paste (Fig. 4c). For PVP-based 65 : 35 systems, the final recovery of the low molar mass paste was 211 ± 5%, and the recovery of the high molar mass paste was 700 ± 100% (Fig. 4d). All pastes exhibit over 100% recovery, indicating that the post-shear storage modulus is greater than its original value. Thixotropic recovery beyond the original storage modulus is not commonly observed in dense pastes, but has been reported by Shakell *et al.* and is attributed to network densification.[62,66] Network densification in these tests is indicative of significant rearrangements of the particle spatial distribution (microstructure) during shear and aging.

For both PEO and PVP polymer binders, the high molar mass systems show a deviation from 100% that is more than twice that of the low molar mass systems. Similar to the settling results, the low molar mass polymer formulations appear to provide an improved resistance against shear-induced development of heterogeneities, in this case showing improved stability against rearrangements of the particle spatial distribution under shear and network densification. Further, it is interesting to note that the low molar mass polymer systems have a final recovery between 150–210% independent of the volume ratio of coarse to fine particles or polymer chemistry, indicating the more stable low molar mass systems are also less sensitive to changes in particle content. This is in contrast to the final recovery of the high molar mass polymer systems that displayed a 140% and 260% increase in total recovery from the 71 : 29 to the 65 : 35 volume ratio of coarse to fine particle systems for the PVP and PEO polymers, respectively.

While thixotropic recovery occurs on short time scales, the evolution of the storage modulus that occurs slowly throughout the recovery period is indicative of aging. Aging is a phenomenon observed in soft glassy systems where the material properties continuously evolve over time instead of reaching a stable value. While perfectly thixotropic materials will reach a constant storage modulus after short time scales (seconds to minutes), soft glassy materials—materials that exhibit a yield stress, thixotropy, and aging[67]—can exhibit a dynamic storage modulus over many hours. In dense pastes, especially with significant concentrations of binders, microstructural rearrangements are hindered and aging is not surprising. Therefore, the initial recovery of the paste's storage modulus after the removal of shear is due to the material's thixotropic response, while the dynamic recovery at longer time scales is due to aging.

The high and low molar mass systems appear to have distinctly different aging behavior throughout the recovery period. All low molar mass formulations display a typical inverse exponential curve, while all high molar mass formulations display an 'S' shaped curve. This is particularly visually notable in Fig. 4c for the high molar mass PEO with the 65 : 35 volume ratio of coarse to fine particles. Several studies that investigate aging behavior have shown that the storage modulus increases logarithmically with time:[68–71]

$$G'(t) \sim t^{\beta} \tag{2}$$

This type of relationship is commonly observed during aging, and phenomenological modeling is often used to study aging in these systems.[72,73] Eqn (2) is used here to quantify dynamic restructuring behavior and reveal how polymer molar mass influences the dynamic mechanisms of heterogeneity formation and restructuring.

Fig. 5 shows the storage modulus' growth over time for high and low molar mass systems at the two coarse to fine particle size ratios during initial rest (G'_0), and during recovery (G') after shearing at 40 s^{-1} for 100 s. The data is plotted on a log–log scale to clearly show the characteristic aging that occurs over the 2-hour recovery period. For all formulations tested, the G'_0 values measured during rest show a stable storage modulus over time before shearing. Linear regression was used to determine β values for all eight formulations. The data was segmented, and Grubbs outlier analysis was used to determine if the logarithmic scaling relationship (β) changed significantly between the different segments, as analyzed throughout the recovery period. This analysis confirmed that low molar mass formulations displayed a gradual growth in the storage modulus over time corresponding to a single β value of 1.17 or 0.92 in systems with the 71 : 29 coarse to fine particle volume ratio and either the PEO or PVP polymer, respectively. Similarly, the single β value observed for the 63 : 35 volume ratio of coarse to fine particles was 1.24 and 1.01 for the low molar mass PEO and PVP polymers, respectively. Interestingly, all high molar mass systems exhibited a significant discrepancy between early and late stage recovery behavior, corresponding to the emergence two distinct recovery stages and β values. This gives rise to the 'S' shaped curves observed in Fig. 4, and can be seen in Fig. 5 as late recovery behavior that has a significantly stronger logarithmic dependence (steeper slope) compared to early recovery times. Although storage modulus aging is not thoroughly understood, prior work suggests it occurs when particles become elastically trapped in high energy states as the microstructure forms, and that major shifts in measured properties are a result of some significant particle restructuring event.[66,71,74–76] This indicates that binder molar mass and concentration not only influence the severity of the particle microstructural rearrangements that occur due to shearing and aging processes, but also fundamentally change the mechanisms of particle restructuring, which we discuss in more detail later.

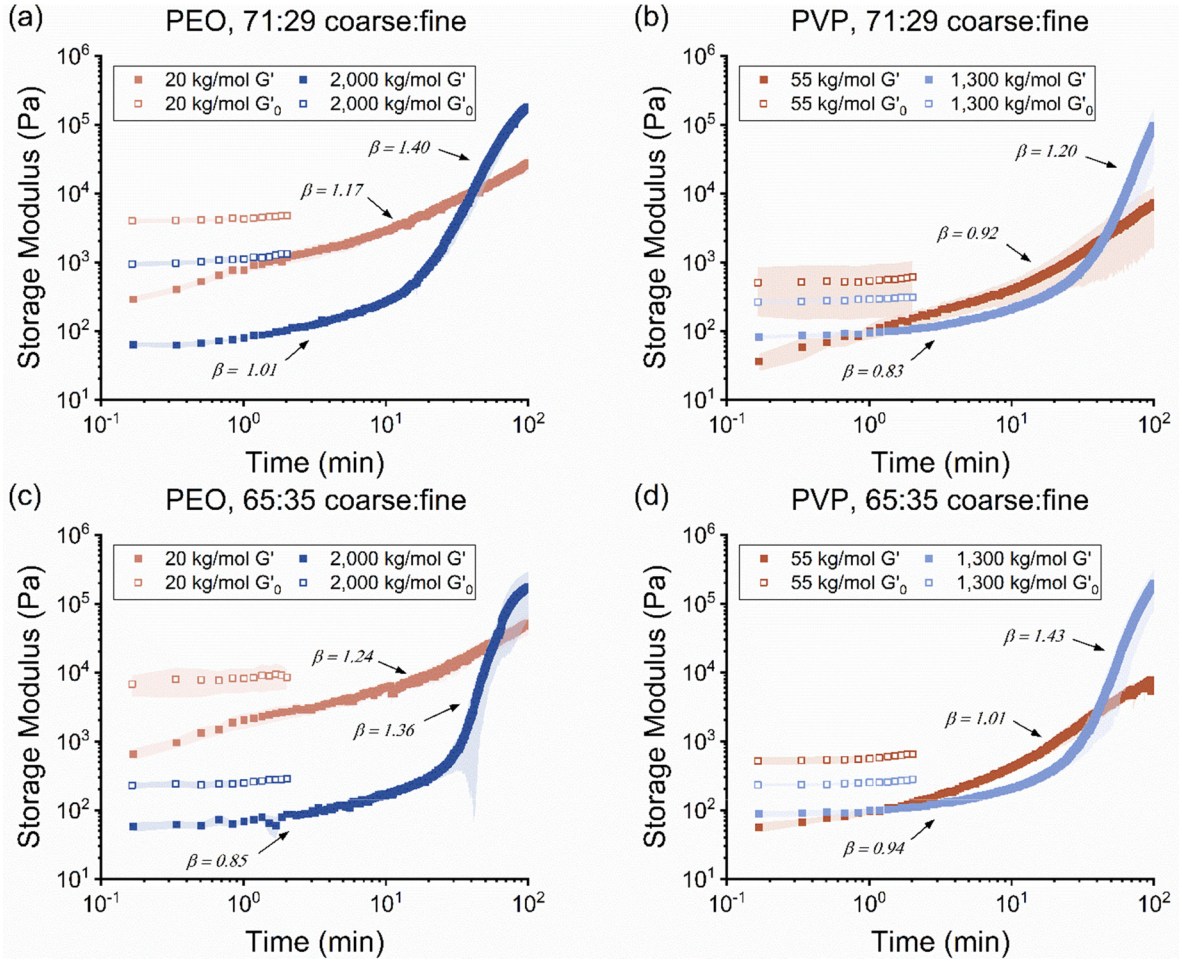

Fig. 5 Aging behavior over time for viscosity matched PEO (a) and (c) and PVP (b) and (d) binders with a 71 : 29 volume ratio of coarse to fine particles (a) and (b) and a 65 : 35 volume ratio of coarse to fine particles (c) and (d). Shaded regions indicate uncertainty to one standard deviation of three replicate measurements. Open symbols represent the storage modulus measured from the initial rest interval (G_0') and closed symbols represent aging data from the recovery interval (G') during 3IT tests.

The observed differences in total storage modulus recovery among the tested formulations demonstrates that molar mass and concentration significantly influence paste rheology, independent of binder viscosity. This is unexpected, as non-colloidal particles are not heavily influenced by molecular interactions due to the length scale of forces at play (micron sized glass beads are significantly larger and heavier than polymer chains). It is unlikely that polymer–particle interactions are responsible for the differences observed between high and low molar mass systems. Instead, it is more likely that the influence of molar mass and concentration is a product of long range hydrodynamic forces, which have been shown to impact heterogeneity formation in less concentrated particle suspensions.[41,77,78] Features of particle movement and microstructure evolution over time, including information regarding the balance of elastic and viscous properties of polymers and dense pastes, may be revealed through small amplitude oscillatory shear (SAOS) sweeps.[62] SAOS sweeps were performed to gain insights into the viscoelastic properties of the pastes.

Tan(δ) represents the ratio of viscous and elastic contributions to the material's modulus, G''/G', and is plotted as a function of oscillation amplitude in Fig. 6 (results of G' and G'' *vs.* oscillation amplitude can be found in Fig. S9). The LVR represents the behavior of the material at rest and can be seen at strains below 0.1% where the tan(δ) is low and does not change with applied strain. Lower values of tan(δ) correspond to heightened structural rigidity with values above one representing a higher viscous contribution compared to elastic ($G'' > G'$). All LVR tan(δ) values are greater than or equal to one with PEO systems displaying slightly lower values ranging from approximately 1–2 compared to PVP systems with values of approximately 2.5–3.5. Higher values of tan(δ) within the LVR indicate PVP systems may be weaker compared to PEO ones.

Yielding can be seen in all formulations and occurs at the point when tan(δ) begins to increase with applied strain. The yielding transition occurs at strains of approximately 0.1–0.3% and represents the breakdown of the particle microstructure. Interestingly, although the yield strain is similar across the different formulations, the nature of the yielding transition is

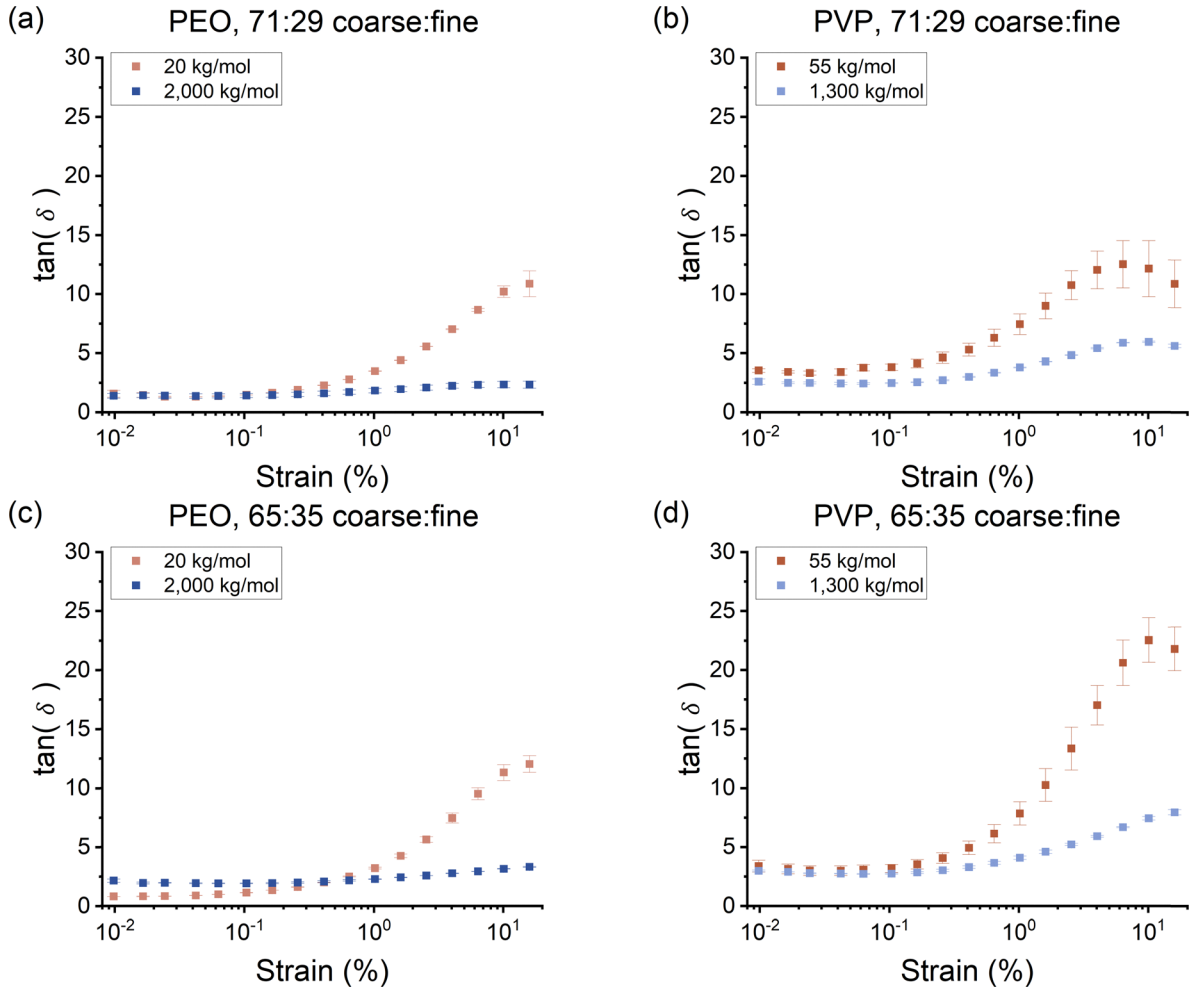

Fig. 6 Tan(δ) as a function of oscillation amplitude for viscosity matched PEO (a) and (c) and PVP (b) and (d) binders with a coarse to fine particle volume ratio of 71 : 29 (a) and (b) and 65 : 35 (c) and (d). Error bars represent uncertainty to one standard deviation from three replicate measurements.

significantly different between the high and low molar mass systems. Low molar mass systems display a relatively sharper increase to higher tan(δ) values at deformations exceeding the yield strain. This is most apparent in the PEO formulations as the tan(δ) for the high molar mass systems remains below five at all strains tested. The heightened tan(δ) values indicate that low molar mass systems yield more viscously compared to their high molar mass counterparts.

Discussion

Overall, it is evident that low molar mass polymer systems are more stable against settling and shear induced migration/aging effects compared to their high molar mass counterparts for a given viscosity of the binder solution. To prevent settling and segregation, particles must either form load-bearing structures that are stable against gravity or shear, or the polymer must absorb onto the particles to effectively provide a load-bearing coating layer that can resist gravity or shear. Polymer adsorption is possible in these systems, but unlikely to influence the settling of non-colloidal particles. This implies that the structures formed in high molar mass systems are insufficiently load bearing and undergo densification, resulting in binder segregation under gravitational forces and evidence of heterogeneity formation under shear and aging. This framework is consistent with the two-stage recovery behavior observed in high molar mass systems during aging (Fig. 5). Two-stage recovery is characteristic of the formation of metastable structures in the first stage that eventually collapse, resulting in the emergence of a second stage where the particle structure undergoes densification.[70] Therefore, the improved stability against settling and shear-induced restructuring observed in low molar mass systems may be attributed to the formation of stable, load-bearing particle structures.

SAOS experiments are a good indicator of particle structures and deformations, as they probe the viscous and elastic properties of a material under the small-scale deformations that occur during settling and recovery. Fig. 6 shows that the low molar mass systems have more viscous yielding at low strains while the yielding behavior of the high molar mass systems is relatively more elastic, as indicated by lower tan(δ) values. Yielding occurs

when particles are irreversibly displaced from their original positions, and a high tan(δ) upon yielding indicates that shearing forces are viscously dissipated. Viscous dissipation may be a feature of particle structures that are able deform into low energy state, stable structures during recovery and settling, and has been related to improved print quality during extrusion processes.[79] This is particularly apparent for the high molar mass PEO systems, which have the lowest tan(δ) values upon yielding and also display the most binder segregation during settling. Particles that are not viscously displaced under applied forces will be elastically constrained, possibly in metastable states or heterogeneous structures that form during shearing. This points to complex interactions between materials in these mixtures, such as polymer-particle interactions or lubrication effects, which drive the observed behaviors. This evidence suggests viscous yielding is important to dense paste stability in the presence of polymer solution binders.

Previous studies have also shown that a lack of elasticity, particularly within the LVR, can result in poor structural strength and thus stability.[80] The LVR tan(δ) is an indicator of structural strength with high tan(δ) values being indicative of structures that lack elasticity and may not be load bearing. Indeed, the most stable low molar mass PEO systems displayed high elasticity within the LVR as well as viscous yielding. It is possible that the heightened LVR tan(δ) observed for PEO systems may be attributed to polymer elasticity as aqueous solutions of PEO are known to be highly elastic.[49] The fact that viscous yielding is more pronounced in low molar mass systems may be a result of lubrication effects as low molar mass polymers have been shown to have improved mobility and lubrication, even in viscosity matched systems.[81,82] The difference in sedimentation rates between viscosity matched systems could therefore be attributed to viscoelasticity and lubrication effects, which are not factored into Newtonian based hindered settling models. While further experimentation is required to confirm this relationship, our analysis is consistent with prior findings and indicates that these attributes play a key role in dense paste stability.

Finally, it should be noted that varying the coarse to fine particle volume ratio primarily affected the stability of dense pastes formulated with high molar mass polymer binders. This likely occurs because the fine particles are smaller and less massive compared to the coarse particles and therefore contribute little to the formation of load bearing structures primarily consisting of large particles.[83,84] In contrast, pastes formulated with low molar mass binders exhibited stable structures even at elevated fine particle contents. While this trend is most evident under shear, it is less pronounced in settling tests. These results suggest that the stabilizing effects of low molar mass binders can counteract the destabilizing effects associated with increasing fine particle content, depending on the magnitude of the forces at play.

Conclusions

This study investigates the effects of binder polymer molar mass and concentration as well as fine particle content on the stability of dense pastes. Paste stability was characterized by the resistance to binder segregation under gravitational forces as well as resistance to irreversibly rearranging when sheared. Viscosity-matched binders were used to isolate the effects of polymer molar mass and concentration and revealed that, in general, pastes formulated with high molar mass polymers at low concentrations were more prone to heterogeneity formation compared to low molar mass polymers at higher concentrations. This is attributed to enhanced viscous yielding in low molar mass high concentration fluids, which was revealed through SAOS sweeps. We hypothesize viscous yielding allows particles to viscously deform into low energy state, homogeneous, particle dispersions while the absence of viscous yielding means that particles may be trapped in high energy state, heterogeneous dispersions. Additionally, we find that increasing fine particle content either increases the severity of heterogeneity formation or has no effect. This is likely because fine particles are significantly smaller and less massive compared to large particles and do not meaningfully contribute to the formation of stable microstructures.

Given that heterogeneity formation is a known and often unavoidable consequence of paste processing, this work offers a meaningful contribution toward its minimization. Though developed with specific polymer systems and particle types, the findings are likely generalizable across other non-colloidal paste formulations with similar particle packing properties. Although long chain polymers are typically desirable for their solid-state mechanical properties, these studies highlight the fact that formulating pastes with long chain polymers may result in heterogeneities in the particle microstructure, which can ultimately hinder the mechanical strength and performance of the final composite. These insights contribute to ongoing efforts to minimize heterogeneity formation during composite processing and may aid in the formulation of more robust, defect-tolerant pastes for applications in additive manufacturing, coatings, and beyond.

Conflicts of interest

There are no conflicts to declare.

Data availability

The data supporting this article have been included as part of the supplementary information (SI). Supplementary information is available. See DOI: https://doi.org/10.1039/d5sm01059d.

Acknowledgements

This work was funded by Office of Naval Research (N000142212031). AD also acknowledges the Department of Education Graduate Assistance in Areas of National Need (GAANN) program (P200A210037).

References

1 A. Shen, PhD thesis, University of Connecticut, 2018.
2 M. Tidau and J. H. Finke, *RPS Pharm. Pharmacol. Rep.*, 2024, **3**, rqae007.
3 D. J. Kline, M. D. Grapes, E. A. Avalos, C. M. Landeros, H. P. Martinez, R. V. Reeves, K. T. Sullivan and Z. D. Doorenbos, *Powder Technol.*, 2022, **411**, 117947.
4 A. Perrot, D. Rangeard and A. Pierre, *Mater. Struct.*, 2016, **49**, 1213–1220.
5 A. E. Marnot, A. A. Dobbs and B. K. Brettmann, *MRS Commun.*, 2022, **12**, 483–494.
6 A. Marnot, K. Koube, S. Jang, N. Thadhani, J. Kacher and B. Brettmann, *Virtual Phys. Prototyping*, 2023, **18**, e2279149.
7 H. A. Barnes, *J. Rheol.*, 1989, **33**, 329–366.
8 S. C. Tsai, D. Botts and J. Plouff, *J. Rheol.*, 1992, **36**, 1291–1305.
9 D. I. Wilson and S. L. Rough, *Chem. Eng. Sci.*, 2006, **61**, 4147–4154.
10 M. M. Rueda, M.-C. Auscher, R. Fulchiron, T. Périé, G. Martin, P. Sonntag and P. Cassagnau, *Prog. Polym. Sci.*, 2017, **66**, 22–53.
11 H. Woods, A. Boddorff, E. Ewaldz, Z. Adams, M. Ketcham, D. J. Jang, E. Sinner, N. Thadhani and B. Brettmann, *Propellants, Explos., Pyrotech.*, 2020, **45**, 26–35.
12 L. Jian, C. Zhou, W. Gang, Y. Wei, T. Ying and L. Qing, *Polym. Compos.*, 2003, **24**, 323–331.
13 K. Yin, A.-L. Fauchille, E. Di Filippo, P. Kotronis and G. Sciarra, *Geotechnics*, 2021, **1**, 260–306.
14 I. Campbell, A. Marnot, M. Ketcham, C. Travis and B. Brettmann, *AIChE J.*, 2021, **67**, e17412.
15 D. M. Kalyon and S. Aktaş, *Annu. Rev. Chem. Biomol. Eng.*, 2014, **5**, 229–254.
16 D. M. Kalyon, D. Dalwadi, M. Erol, E. Birinci and C. Tsenoglu, *Rheol. Acta*, 2006, **45**, 641–658.
17 D. M. Kalyon and H. N. Sangani, *Polym. Eng. Sci.*, 1989, **29**, 1018–1026.
18 S. Jang, A. Boddorff, D. J. Jang, J. Lloyd, K. Wagner, N. Thadhani and B. Brettmann, *Addit. Manuf.*, 2021, **47**, 102313.
19 D. Behera and M. Cullinan, *Precis. Eng.*, 2021, **68**, 326–337.
20 ed. M. J. Mezger, K. J. Tindle, M. Pantoya, L. J. Groven and D. Kalyon, *Energetic Materials: Advanced Processing Technologies for Next-Generation Materials*, CRC Press, Boca Raton, 2017.
21 T. S. Shivashankar, R. K. Enneti, S.-J. Park, R. M. German and S. V. Atre, *Powder Technol.*, 2013, **243**, 79–84.
22 K. Rane, L. Di Landro and M. Strano, *Powder Technol.*, 2019, **345**, 553–562.
23 I. Ochoa and S. G. Hatzikiriakos, *Powder Technol.*, 2005, **153**, 108–118.
24 J. R. Abbott, N. Tetlow, A. L. Graham, S. A. Altobelli, E. Fukushima, L. A. Mondy and T. S. Stephens, *J. Rheol.*, 1991, **35**, 773–795.
25 L. A. Mondy, A. L. Graham, J. R. Abbott and H. Brenner, Los Alamos National Lab. (LANL), Los Alamos, NM (United States), Argonne, IL, 1993.
26 P. Mirbod and N. C. Shapley, *J. Rheol.*, 2023, **67**, 417–432.
27 D. Leighton and A. Acrivos, *J. Fluid Mech.*, 1987, **181**, 415–439.
28 D. Leighton and A. Acrivos, *J. Fluid Mech.*, 1987, **177**, 109–131.
29 A. S. Kondrat'ev and E. A. Naumova, *Theor. Found. Chem. Eng.*, 2008, **42**, 96–101.
30 J. F. Richardson and W. N. Zaki, *Chem. Eng. Res. Des.*, 1997, **75**, S82–S100.
31 A. S. Kondrat'ev and E. A. Naumova, *Theor. Found. Chem. Eng.*, 2006, **40**, 387–392.
32 P. Mandakini, B. Sowmya, M. Anand and M. Narasimha, *Trans. Indian Inst. Met.*, 2020, **73**, 2089–2095.
33 P. Snabre, B. Pouligny, C. Metayer and F. Nadal, *Rheol. Acta*, 2009, **48**, 855–870.
34 D. Lerche, *KONA Powder Part. J.*, 2019, **36**, 156–186.
35 A. Potanin, *Colloids Surf. Physicochem. Eng. Asp.*, 2019, **562**, 54–60.
36 U. Yilmazer, C. G. Gogos and D. M. Kalyon, *Polym. Compos.*, 1989, **10**, 242–248.
37 K. M. Hill, D. V. Khakhar, J. F. Gilchrist, J. J. McCarthy and J. M. Ottino, *Proc. Natl. Acad. Sci. U. S. A.*, 1999, **96**, 11701–11706.
38 J. He, S. S. Lee and D. M. Kalyon, *J. Rheol.*, 2019, **63**, 19–32.
39 M. Cloitre and R. T. Bonnecaze, *Rheol. Acta*, 2017, **56**, 283–305.
40 D. Won and C. Kim, *J. Non-Newton. Fluid Mech.*, 2004, **117**, 141–146.
41 E. Pererson, PhD thesis, Georgia Institute of Technology, 2013.
42 V. Breedveld, PhD thesis, University of Twente, 2000.
43 D. A. Clarke, W. Hogendoorn, A. Penn and M. R. Serial, *Particuology*, 2025, **101**, 18–32.
44 C. Ness, R. Seto and R. Mari, *Annu. Rev. Condens. Matter Phys.*, 2022, **13**, 97–117.
45 F. Gauthier, H. L. Goldsmith and S. G. Mason, *Rheol. Acta*, 1971, **10**, 344–364.
46 M. M. Gumulya, R. R. Horsley, V. Pareek and D. D. Lichti, *Chem. Eng. Sci.*, 2011, **66**, 5822–5831.
47 S. Mora, L. Talini and C. Allain, *Phys. Rev. Lett.*, 2005, **95**, 088301.
48 M. A. Tehrani, *J. Rheol.*, 1996, **40**, 1057–1077.
49 G. D'Avino, G. Romeo, M. M. Villone, F. Greco, P. A. Netti and P. L. Maffettone, *Lab Chip*, 2012, **12**, 1638–1645.
50 G. Ovarlez, F. Mahaut, S. Deboeuf, N. Lenoir, S. Hormozi and X. Chateau, *J. Rheol.*, 2015, **59**, 1449–1486.
51 S. Dagois-Bohy, S. Hormozi, É. Guazzelli and O. Pouliquen, *J. Fluid Mech.*, 2015, **776**, R2.
52 R. D. Corder, Y.-J. Chen, P. Pibulchinda, J. P. Youngblood, A. M. Ardekani and K. A. Erk, *Soft Matter*, 2023, **19**, 882–891.
53 T. A. Prabhu and A. Singh, *Rheol. Acta*, 2021, **60**, 107–118.
54 N. Adjou, A. Yahia, M. N. Oudjit and M. Dupuis, *Constr. Build. Mater.*, 2022, **327**, 126980.
55 K. Bekkour, M. Leyama, A. Benchabane and O. Scrivener, *J. Rheol.*, 2005, **49**, 1329–1345.
56 C. W. Macosko and R. G. Larson, *Rheology: principles, measurements, and applications*, VCH, New York, NY, 1994.

57 C. Zhu and J. E. Smay, *J. Rheol.*, 2011, **55**, 655–672.
58 Y. Eom, F. Kim, S. E. Yang, J. S. Son and H. G. Chae, *J. Rheol.*, 2019, **63**, 291–304.
59 B. Nan, P. Gołębiewski, R. Buczyński, F. J. Galindo-Rosales and J. M. F. Ferreira, *Materials*, 2020, **13**, 1636.
60 Y. E. Pivinskii, *Refractories*, 1987, **28**, 537–545.
61 K. Kondepudi and K. V. L. Subramaniam, *Cem. Concr. Compos.*, 2021, **119**, 103983.
62 A. Shakeel, A. Kirichek and C. Chassagne, *Mar. Pet. Geol.*, 2020, **116**, 104338.
63 H. Brenner, S. A. Altobelli, A. L. Graham, J. R. Abbott and L. A. Mondy, in *Theoretical and Applied Rheology*, ed P. Moldenaers and R. Keunings, Elsevier, Amsterdam, 1992, pp. 585–587.
64 C. Mobuchon, P. J. Carreau and M.-C. Heuzey, *Rheol. Acta*, 2007, **46**, 1045–1056.
65 M. K. Lyon, D. W. Mead, R. E. Elliott and L. G. Leal, *J. Rheol.*, 2001, **45**, 881–890.
66 H. Van Damme, S. Mansoutre, P. Colombet, C. Lesaffre and D. Picart, *C. R. Phys.*, 2002, **3**, 229–238.
67 P. Coussot, *Soft Matter*, 2007, **3**, 528–540.
68 R. Bandyopadhyay, D. Liang, J. L. Harden and R. L. Leheny, *Solid State Commun.*, 2006, **139**, 589–598.
69 J. Ren, B. F. Casanueva, C. A. Mitchell and R. Krishnamoorti, *Macromolecules*, 2003, **36**, 4188–4194.
70 M. A. Treece and J. P. Oberhauser, *Polymer*, 2007, **48**, 1083–1095.
71 M. A. Treece and J. P. Oberhauser, *Macromolecules*, 2007, **40**, 571–582.
72 S. M. Fielding, M. E. Cates and P. Sollich, *Soft Matter*, 2009, **5**, 2378–2382.
73 C. Derec, G. Ducouret, A. Ajdari and F. Lequeux, *Phys. Rev. E:Stat., Nonlinear, Soft Matter Phys.*, 2003, **67**, 061403.
74 M. B. Gordon, C. J. Kloxin and N. J. Wagner, *Soft Matter*, 2021, **17**, 924–935.
75 Y. M. Joshi, *Soft Matter*, 2015, **11**, 3198–3214.
76 R. Radhakrishnan, T. Divoux, S. Manneville and S. M. Fielding, *Soft Matter*, 2017, **13**, 1834–1852.
77 D. Jin, J. I. Park, J. B. You, Y. Kim, H. Lee and J. M. Kim, *J. Fluid Mech.*, 2025, **1004**, A5.
78 F. Boyer, O. Pouliquen and É. Guazzelli, *J. Fluid Mech.*, 2011, **686**, 5–25.
79 R. Agrawal and E. García-Tuñón, *Soft Matter*, 2024, **20**, 7429–7447.
80 R. Durairaj, S. Ramesh, S. Mallik, A. Seman and N. Ekere, *Mater. Des.*, 2009, **30**, 3812–3818.
81 L. Ji, A. Orthmann, L. Cornacchia, J. Peng, G. Sala and E. Scholten, *Carbohydr. Polym.*, 2022, **297**, 120000.
82 D. Cangialosi, V. M. Boucher, A. Alegría and J. Colmenero, *Soft Matter*, 2013, **9**, 8619–8630.
83 A. Agrawal, H.-Y. Yu, S. Srivastava, S. Choudhury, S. Narayanan and L. A. Archer, *Soft Matter*, 2015, **11**, 5224–5234.
84 T. Sentjabrskaja, E. Babaliari, J. Hendricks, M. Laurati, G. Petekidis and S. U. Egelhaaf, *Soft Matter*, 2013, **9**, 4524–4533.

